Contrasting features of parton energy loss in heavy-ion collisions at RHIC and LHC*

Thomas Marshall[1†] [iD]   Philip Suh[1,2,3]   Gang Wang (王钢)[1] [iD]   Huan Zhong Huang (黄焕中)[1,4] [iD]

[1]Department of Physics and Astronomy, University of California, Los Angeles, California 90095, USA
[2]Oxford Academy High School, Cypress, California 90630, USA
[3]Stanford University, Stanford, California 94305, USA
[4]Key Laboratory of Nuclear Physics and Ion-beam Application (MOE), and Institute of Modern Physics, Fudan University, Shanghai 200433, China

Abstract: Energetic quarks and gluons lose energy as they traverse the hot and dense medium created in high-energy heavy-ion collisions at the BNL Relativistic Heavy Ion Collider (RHIC) and CERN Large Hadron Collider (LHC). The nuclear modification factor (R_{AA}) of leading particles quantifies parton energy loss in such collisions, with the particle spectrum in $p+p$ collisions as a reference. Previous R_{AA} measurements at RHIC energies have revealed an approximately constant trend at high transverse momenta (p_T), implying a scenario where parton energy loss, Δp_T, scales proportionally with p_T, a feature naively expected from energy loss dynamics in elastic collisions. In this study, we investigate the LHC R_{AA} measurements that exhibit a pronounced p_T dependence of R_{AA} for various particle species, and our analysis attributes this behavior to Δp_T being approximately proportional to $\sqrt{p_T}$. These distinct features are consistent with model calculations of dominant radiative energy loss dynamics at LHC, in contrast to the dominance of collisional energy loss at RHIC. Additionally, the linear increase of the fractional energy loss with medium density at different p_T magnitudes affirms our previous empirical observation that the magnitude of the energy loss depends more strongly on the initial entropy density than the parton's path length through the medium. Implications on the dynamical scenarios of parton energy loss and future experimental investigations are also discussed.

Keywords: heavy-ion collision, nuclear modification factor, parton energy loss

I. INTRODUCTION

Color opacity stands as a fundamental trait of the hot and dense medium created in heavy-ion collisions at the BNL Relativistic Heavy Ion Collider (RHIC) and CERN Large Hadron Collider (LHC). As energetic quarks and gluons traverse the medium, they shed energy through elastic scattering [1−4] and radiation of soft gluons [5−7]. In the scenario of an infinitely-high-momentum parton or infinitely massive scattering center, energy loss would predominantly occur through radiative processes. Conversely, in the opposite scenario, collisional energy loss would become the dominant factor. Prior empirical examinations of final-state leading particle spectra and the pertinent nuclear effects, using RHIC data, have revealed the proportionality between parton energy loss (Δp_T) and the magnitude of transverse momentum (p_T) [8−10]. Although most theoretical energy loss calculations at RHIC

are framed through the lens of radiative energy loss [11, 12], a proportional relationship between parton energy loss and transverse momentum tends to correspond better with a "classical mechanics" understanding of elastic scattering and collisional energy loss, where higher-momentum bodies tend to lose proportionally more energy in collisions. Previous theoretical predictions additionally seem to show a linear dependence of the energy loss on the energy magnitude for heavy quarks, which would align with a similar dependence on p_T [3].

Given that collision center-of-mass energies ($\sqrt{s_{NN}}$) at LHC significantly surpass those at RHIC by over an order of magnitude, the associated p_T range of generated particles now spans into a realm where radiative energy loss dynamics are expected to assume a more prominent role. Parton energy loss under the LHC center-of-mass energy regime has previously been studied through the analysis of jet suppression S_{loss} results with ATLAS [13],

but performing a similar study using leading particles instead allows for a cleaner look into the magnitude and p_T dependence of the energy loss without some compounding effects within jets. If energy loss and fragmentation were to occur sequentially − where fragmentation takes place outside the medium after the leading parton loses energy within the medium − leading particles would provide a clearer means of investigation than jets. Recent theoretical simulations of jet-induced medium excitation have examined the diffusion wake in high-p_T jet-photon pairs and predicted an identical width both with and without accounting for the medium, suggesting the possibility of separating energy loss and fragmentation [14]. Hence, the analysis of LHC data using the same framework as in Ref. [8] is warranted to investigate the potential transition in the dynamics of energy loss from RHIC to LHC through the study of leading particle data instead of jet data.

Both radiative and collisional energy losses are intricately linked to the path length (L) and entropy density of the medium. We approximate the medium entropy density as $\frac{1}{S}\frac{dN}{dy}$, where $\frac{dN}{dy}$ represents the experimentally measured particle density per unit rapidity, and S corresponds to the transverse overlap area of the colliding system, which can be determined using Monte Carlo Glauber calculations [15−18]. A previous study of RHIC data found a minimal dependence of Δp_T on L, implying that parton energy loss is predominantly determined by the initial medium density [8]. This feature could arise from the scenario of rapid expansion of the collision system, resulting in a rapid decrease in medium entropy density over time. It is of great interest to investigate whether the LHC data corroborate the same characteristics.

II. METHOD

In experiments, the nuclear modification factor, R_{AA}, quantifies the suppression or enhancement of particle yields in heavy-ion collisions relative to a nucleon-nucleon (NN) reference:

$$R_{AA}(p_T) = \frac{d^2N^{AA}/dp_T d\eta}{T_{AA}d^2\sigma^{NN}/dp_T d\eta}, \tag{1}$$

where T_{AA} accounts for the nuclear collision geometry, and η denotes pseudorapidity. Both STAR [19–20] and PHENIX [21–22] data demonstrate a plateauing of the R_{AA} spectrum at values much lower than unity in the high-p_T region ($\gtrsim 5$ GeV/c). Treating the suppression of the nuclear modification factor as a result of empirical loss of transverse momentum from the $p+p$ spectrum to the nucleus+nucleus spectrum, these flat R_{AA} curves were found to indicate a constant fractional p_T shift in the spectrum. From a classical standpoint, this behavior is

consistent with elastic collisional energy loss. Higher-p_T particles would lose a proportionally higher amount of momentum through elastic collisions within the medium, resulting in a constant $\Delta p_T/p_T$. While this seems to describe the observed RHIC data fairly well, LHC data demonstrate significantly different characteristics.

Figure 1 plots the published p_T spectra of various final-state particles in $p+p$ collisions at (a) 2.76 TeV and (b) 5.02 TeV. Each dataset can be described by a Tsallis distribution [29]:

$$\frac{1}{2\pi p_T}\frac{d^2N}{dp_T d\eta} = A(1 + \frac{p_T}{p_0})^{-n}, \tag{2}$$

where A, p_0, and n are free parameters in the fit. The fit results for each of these parameters and the χ^2/ndf (number of degrees of freedom) for each fit are listed in Tables
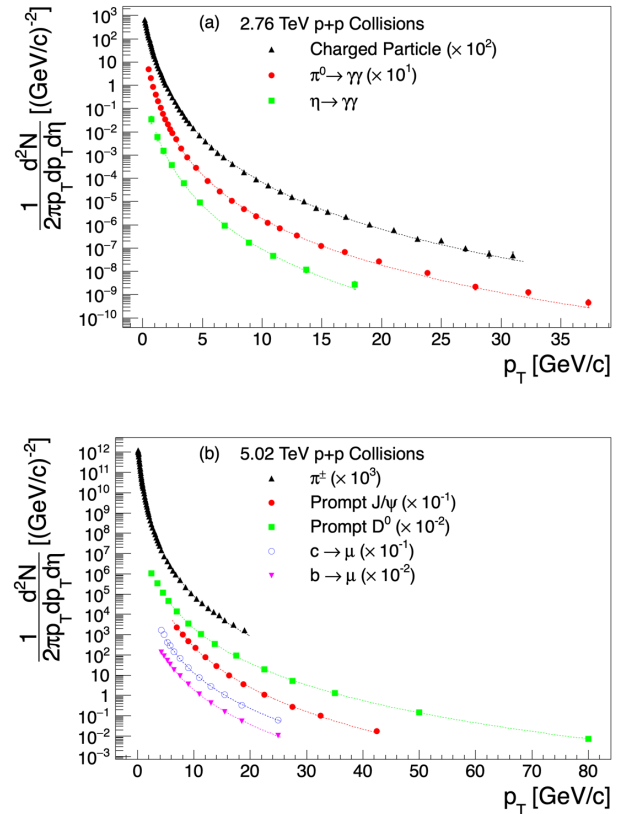

Fig. 1. (color online) Particle p_T spectra in $p+p$ collisions at (a) 2.76 TeV and (b) 5.02 TeV. The 2.76 TeV data (charged particles, π^0, and η) are from ALICE [23, 24]. The 5.02 TeV results include charged pions from ALICE [25], prompt J/ψ and D^0 mesons from CMS [26, 27], and muons from charm and bottom hadrons from ATLAS [28]. Different scaling factors are applied for better visibility. Note that some datasets used differential rapidity instead of pseudorapidity, but this should not affect the relevant physics involved in this study. Fits to the data follow Eq. (2), as discussed in the text.

Table 1. Fit results for the p_T spectra in $p+p$ collisions at $\sqrt{s_{NN}} = 2.76$ TeV from Fig. 1 using Eq. (2).

Data Set	A	p_0	n	χ^2/ndf
charged particle	4097	0.883	7.13	0.52
$\pi^0 \to \gamma\gamma$	312.0	0.696	6.94	0.82
$\eta \to \gamma\gamma$	0.888	1.305	7.47	0.30

Table 2. Fit results for the p_T spectra in $p+p$ collisions at $\sqrt{s_{NN}} = 5.02$ TeV from Fig. 1 using Eq. (2).

Data Set	A	p_0	n	χ^2/ndf
$\pi^{\pm}$	2.94×10^{12}	0.895	6.97	0.82
prompt J/ψ	6.33×10^{9}	0.987	7.08	0.46
prompt D^0	4.46×10^{8}	1.759	6.47	0.07
$c \to \mu$	5.41×10^{7}	0.957	6.25	0.13
$b \to \mu$	4.40×10^{5}	1.699	6.40	0.73

1 and 2.

Following the procedures outlined in Ref. [8] and treating the suppression empirically as a horizontal shift in the p_T spectrum from $p+p$ to $A+A$ collisions, we can express R_{AA} as

$$R_{AA}(p_T) = \frac{(1 + p'_T/p_0)^{-n} p'_T}{(1 + p_T/p_0)^{-n} p_T} \left[1 + \frac{dS(p_T)}{dp_T} \right], \qquad (3)$$

where $p'_T \equiv p_T + S(p_T)$, and $S(p_T)$ is the magnitude of the shift.

The included factor of $1 + \dfrac{dS(p_T)}{dp_T}$ accounts for the necessary Jacobian term, as mentioned in [13]. Although $S(p_T)$ being proportional to p_T adequately describes RHIC data in the high-p_T region, we start with a more general form in this paper, namely, $S(p_T) = S_0 p_T^{\alpha}$. Then, Eq. (3) becomes

$$R_{AA}(p_T) = \frac{[1 + (p_T + S_0 p_T^{\alpha})/p_0]^{-n}(p_T + S_0 p_T^{\alpha})}{(1 + p_T/p_0)^{-n} p_T}$$
$$\times (1 + S_0 \alpha p_T^{\alpha-1}). \qquad (4)$$

Once we determine p_0 and n for each particle species from the p_T distribution in Fig. 1, we regard them as fixed parameters in Eq. (4) and use this formula to fit the corresponding R_{AA} data, allowing S_0 and α to vary as free parameters.

The necessity of introducing the α parameter is convincingly illustrated in Fig. 2, which shows the R_{AA} measurements as a function of p_T for charged hadrons in Au + Au collisions at 200 GeV [19] and for charged pions in Pb+Pb collisions at 5.02 TeV [25] for the (a) 0–5% and (b) 30%–40% centrality ranges. The fit functions adhere
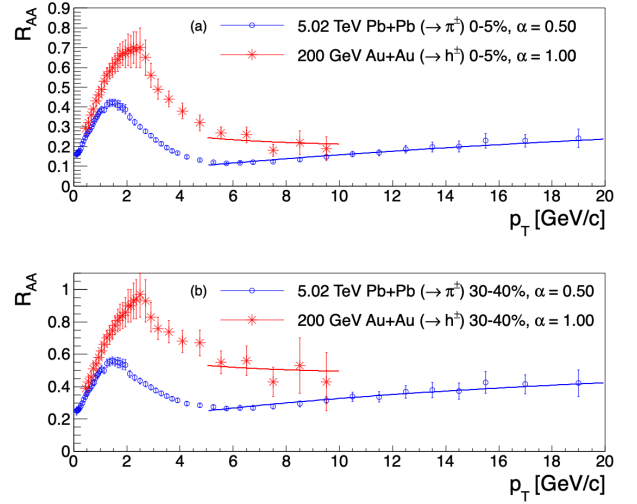

Fig. 2. (color online) R_{AA} as a function of p_T for charged hadrons in Au+Au collisions at 200 GeV (red) [19] and for charged pions in Pb + Pb collisions at 5.02 TeV (blue) [25] for (a) 0–5% and (b) 30%–40% centrality ranges. The fit functions follow Eq. (4) with fixed α values of 1 and 0.5 for RHIC and LHC data, respectively. The corresponding p_0 and n values for the LHC data are extracted from the Tsallis fits in Fig. 1, and those for the RHIC data are taken from Ref. [8].

to Eq. (4), with S_0 serving as the sole free parameter. At $p_T \gtrsim 5$ GeV/c, the flat R_{AA} patterns at RHIC agree with $\alpha = 1$, whereas the increasing trends at LHC harmonize with $\alpha = 0.5$. At both collision energies, the flattening and increasing trends initiate at approximately the same p_T value of approximately 5 GeV/c. This pattern is also evident in the R_{AA} data for other particle species to be presented, presumably because below this p_T, the soft physics dynamics, including hydrodynamics and coalescence formation, dominate, whereas above a p_T of 5 GeV/c, parton fragmentation starts to dominate particle production where the parton energy loss picture emerges.

III. RESULTS

Figure 3 delineates $R_{AA}(p_T)$ for charged hadrons in (a) 0–5% and (b) 30%–40% Pb + Pb collisions at 2.76 TeV [30] and for charged pions in (c) 0–5% and (d) 30%–40% Pb+Pb collisions at 5.02 TeV [25]. All the datasets exhibit upward trends for $p_T \gtrsim 5$ GeV/c. When we apply the same fitting approach and fix α at 0.5, the resulting fit curves (dashed lines) adequately capture all the data points. When we take α as a free parameter (solid curve), the extracted α values are consistent with those for $\alpha=0.5$ within statistical uncertainties. The fit results for all R_{AA} in this study and the corresponding χ^2/ndf are listed in Tables 3 and 4.

We further investigate whether other final-state leading particles also exhibit these features. Fig. 4 shows similar rising trends of R_{AA} at higher p_T for (a) π^0 and (b) η
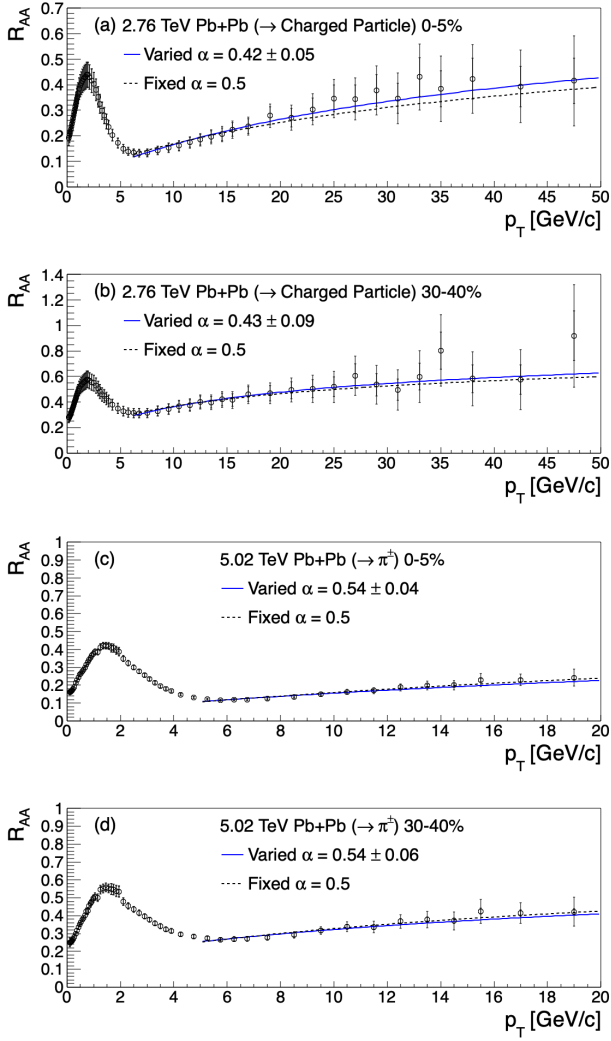
Fig. 3. (color online) $R_{AA}(p_T)$ for charged hadrons in (a) 0–5% and (b) 30%–40% Pb+Pb collisions at 2.76 TeV [30] and for charged pions in (c) 0–5% and (d) 30%–40% Pb+Pb collisions at 5.02 TeV [25]. The fit functions from Eq. (4) either take α as a free parameter or fix it at 0.5, using the p_0 and n values extracted from the Tsallis fits in Fig. 1.

mesons in 0–10% Pb+Pb at 2.76 TeV [31], for (c) prompt J/ψ mesons in 0–100% Pb+Pb at 5.02 TeV [27], and for (d) prompt D^0 mesons in 0–10% Pb+Pb at 5.02 TeV [26]. The α values extracted for π^0, η, and J/ψ mesons are consistent with 0.5 within the fitted statistical uncertainties. The fits to the prompt D^0 data seem to show some tension between the varied and fixed α values, but the significance of the deviation is only 1.6σ. The fixed-parameter fit with $\alpha = 0.5$ agrees with nearly all the D_0 data points within uncertainties. Low precision beyond our R_{AA} fit range in p_T for RHIC data makes it difficult to determine whether the observed $\alpha = 0.5$ versus 1 behavior would also occur for heavy flavor leading particles. However, we would expect this to be the case. Reference [32] presents various transport model studies incorporat-

Table 3. Fit results for $R_{AA}(p_T)$ in Pb + Pb collisions at $\sqrt{s_{NN}}$ = 2.76 TeV from Figs. 3 and 4 using Eq. (4).

Data Set	S_0	α	χ^2/ndf
charged particle (0−5%)	1.56	0.42	0.18
charged particle (30%−40%)	0.80	0.43	0.51
π^0 (0−10%)	1.44	0.50	0.11
η (0−10%)	1.73	0.41	0.08

Table 4. Fit results for $R_{AA}(p_T)$ in Pb + Pb collisions at $\sqrt{s_{NN}}$ = 5.02 TeV from Figs. 3, 4, and 5 using Eq. (4).

Data Set	S_0	α	χ^2/ndf
$\pi^{\pm}$ (0−5%)	1.34	0.54	0.73
$\pi^{\pm}$ (30%−40%)	0.75	0.54	0.37
prompt J/ψ (0−100%)	0.76	0.54	0.30
prompt D^0 (0−10%)	2.36	0.27	0.24
$c \to \mu$ (0−10%)	0.48	0.83	0.20
$b \to \mu$ (0−10%)	0.96	0.60	0.04

ing different energy loss mechanisms, which show good agreement with current RHIC and LHC data. Notably, the Duke model extends the standard Langevin equation by including medium-induced gluon radiation effects, successfully predicting R_{AA} values consistent with observed D meson suppression at LHC. Future high-precision D^0 R_{AA} measurements at high p_T from both LHC and RHIC will be crucial for further constraining the value of α.

Figure 5 displays $R_{AA}(p_T)$ for muons originating from (a) charm and (b) bottom hadrons in 0–10% Pb+Pb collisions at 5.02 TeV. In both cases, the fit curves with $\alpha = 0.5$ align with all data points within uncertainties. The α values extracted from the free-parameter fits exhibit a slight deviation from 0.5, with less than 1.5σ significance. Decay kinematics likely play a role in the smearing of the particle spectra for these cases, which may explain why the α values extracted for the muon data seem to trend above the 0.5 value we observe for the other data studied here.

IV. DISCUSSION

To recap, the analyzed LHC data here suggest that, to explain the R_{AA} measurements for light- and heavy-quark hadrons as a p_T shift in the spectrum from $p+p$ collisions, we require the corresponding Δp_T to scale with $\sqrt{p_T}$. This p_T dependence contrasts with the previously observed proportionality with p_T in RHIC data. Our analysis results with more recent data are in line with a previous study of LHC R_{AA} data that determined the α value to be 0.55 [33]. Our p_T dependence of the parton energy loss at LHC supports theoretical predictions involving energy loss dynamics from medium-induced gluon radi-
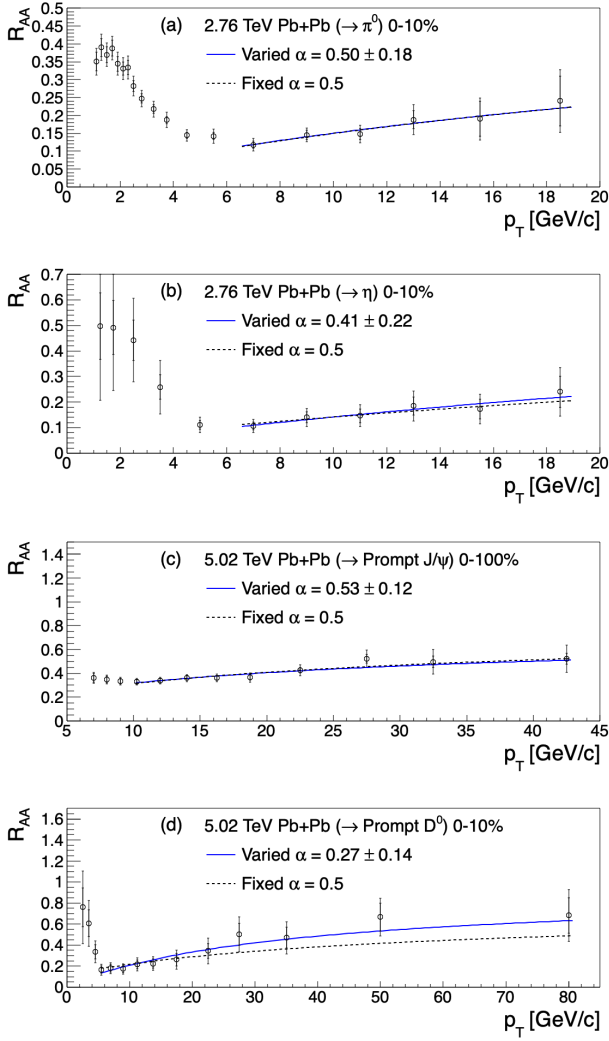
Fig. 4. (color online) $R_{AA}(p_T)$ for (a) π^0 and (b) η mesons in 0–10% Pb+Pb collisions at 2.76 TeV [31], for (c) prompt J/ψ mesons in 0–100% Pb+Pb collisions at 5.02 TeV [27], and for (d) prompt D^0 mesons in 0–10% Pb+Pb collisions at 5.02 TeV [26]. The fit functions from Eq. (4) either take α as a free parameter or fix it at 0.5, using the p_0 and n values extracted from the Tsallis fits in Fig. 1.

Fig. 5. (color online) $R_{AA}(p_T)$ for muons from (a) charm and (b) bottom hadrons in 0–10% Pb+Pb collisions at 5.02 TeV [28]. The fit functions from Eq. (4) either take α as a free parameter or fix it at 0.5, using the p_0 and n values extracted from the Tsallis fits in Fig. 1.

ation [34]. Thus, the distinct change from $\alpha = 1$ at RHIC to $\alpha = 0.5$ at LHC suggests a transition in the relative importance of collisional energy loss dynamics to radiative energy loss dynamics.

This transition in the parton energy loss dynamics within the medium might also give an explanation for the effects of the jet-medium running coupling constant. Theoretical treatment of running coupling effects in both the radiative and elastic contributions to energy loss were previously shown to have robust agreement with LHC and RHIC data for light- and heavy-flavor R_{AA} measurements [35]. In this investigation, the emphasis was placed on the contributions from the radiated gluon vertex to the DGLV integral, particularly noting their significant role
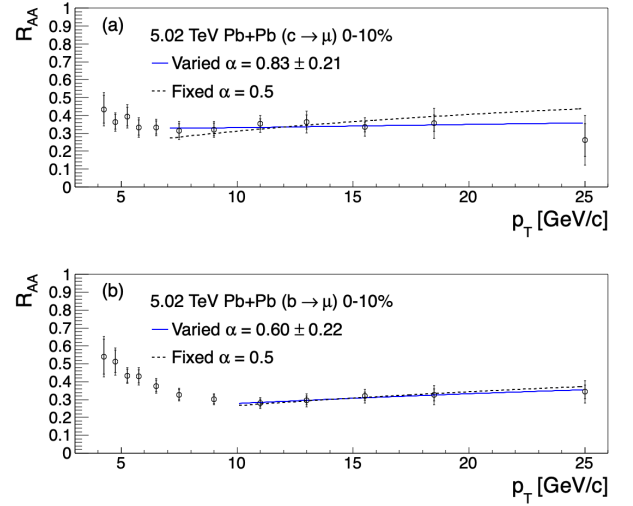
in enhancing the color transparency of the medium for higher-energy jets [35]. Should this apply to leading particles in addition to jets, our conclusion that radiative energy loss has an increased importance at LHC relative to RHIC would be corroborated. While the limited ability to probe a broader p_T spectrum at RHIC may affect the observation of the p_T dependence of the strong coupling constant, we still observe a difference in the R_{AA} trends within the same kinematic range. Within the $p_T \sim 5-10$ GeV/c range, in each collision system shown in Fig. 2, a rising trend is evident in the LHC data but absent in the RHIC data. This observation suggests that the substantial difference in collision energy significantly contributes to this effect, independent of p_T-related effects on α.

The dead cone effect [5] predicts that gluon radiation is more strongly suppressed for bottom quarks than charm quarks, as the former bears a larger mass-to-energy ratio, leading to a wider dead cone. Recent measurements of heavy-quark meson production in $p+p$ collisions by the ALICE experiment [36] reveal heavy-quark fragmentation in the vacuum and provide a direct observation of the dead cone effect. However, the LHC data of the R_{AA} trends for muons from charm and bottom decays do not exhibit the anticipated reduced radiative energy loss for bottom quarks. The decay muon measurements can be influenced by various factors, including substantial momentum smearing resulting from decay kinematics, reduced sensitivity to low-momentum heavy-quark mesons, and the existence of non-prompt $c \to \mu$ decays that originate from b quarks. Recent CMS [37] and ALICE [38] results indicate a significant reduction in the suppression of non-prompt charm hadrons over prompt

charm hadrons, which could, in particular, contribute to the differences we see here via the latter factor. Another factor to consider is that the dead cone effect may become less pronounced for very-high-energy quarks represented in the muon measurements. More precise data are required to elucidate the nature of heavy-quark dynamics in the medium.

In their similar study of S_{loss}, ATLAS additionally investigated the apparent differences in quark and gluon jet suppression by comparing inclusive and photon-tagged jet spectra [13]. These differences were also explored in recent studies of the p_T dispersion of inclusive jets and production cross-sections of J/Ψ mesons [39, 40]. While we do not explore this relationship in our study due to the challenging task of identifying whether our leading particle originates from a quark or gluon, it is crucial to underscore these prior findings and acknowledge their significance in the context of parton energy loss.

However, we do investigate the relationship between energy loss and path length at LHC energies. Previous examinations of RHIC data have revealed that the deduced fractional energy loss, $\Delta p_T/p_T$, is a linear function of medium initial entropy density (quantified by $\frac{1}{S}\frac{\mathrm{d}N}{\mathrm{d}y}$) across different centrality intervals, despite significant variations in the path length for traversing partons [8]. In contrast, when plotted as a function of path length (represented by various parameterizations using the number of participating nucleons N_{part}), $\Delta p_T/p_T$ fails to exhibit a universal trend across different collision systems [8]. This suggests that the initial collision density plays a more significant role in determining parton energy loss than the path length traversed by those partons. We apply the same analysis as adopted in Ref. [8] to the LHC data and discover similar outcomes, as shown in Fig. 6. Because fractional energy loss varies with p_T according to the LHC R_{AA} data, we plot $\Delta p_T/p_T$ as a function of $\frac{1}{S}\frac{\mathrm{d}N}{\mathrm{d}y}$ at different p_T values for charged hadrons in Pb+Pb collisions at 2.76 TeV and for charged pions in Pb+Pb collisions at 5.02 TeV. In each case, for each p_T regime, a clear linear trend emerges, and the linearity is especially strong for higher p_T scales, where parton fragmentation dominates particle production [42].

We also find that the fractional energy loss decreases with increased transverse momentum at LHC energies, agreeing with the trend observed in previous ATLAS S_{loss} measurements for inclusive jets [13], as well as those found in Ref. [42]. The linear trends between $\Delta p_T/p_T$ and $\frac{1}{S}\frac{\mathrm{d}N}{\mathrm{d}y}$ support the previous observation that the initial collision density has a stronger impact than path length, despite the significantly different initial densities at RHIC and LHC. As discussed for RHIC data [8], a subdominant path-length dependence of energy loss might result from the rapid expansion of the medium,
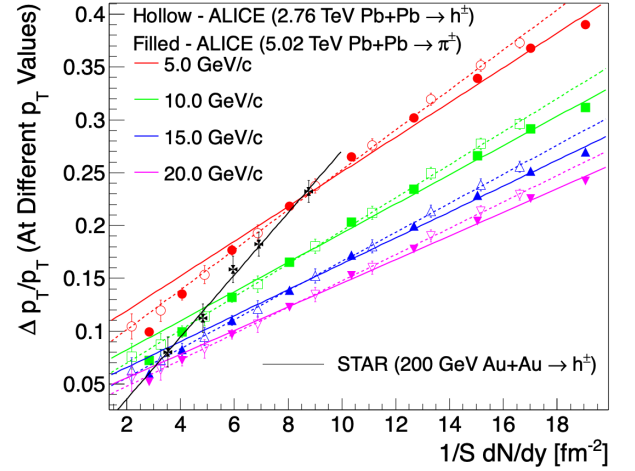

Fig. 6. (color online) Fractional energy loss ($\Delta p_T/p_T$) as a function of centrality (in terms of $\frac{1}{S}\frac{\mathrm{d}N}{\mathrm{d}y}$) based on the analysis in this study and Ref. [8] for charged hadrons in Au+Au collisions at 200 GeV [19] and in Pb + Pb at 2.76 TeV, as well as for charged pions in Pb+Pb at 5.02 TeV. Each of the LHC data points corresponds to a specific p_T value used to calculate fractional energy loss, whereas fractional energy loss has no p_T-dependence in RHIC data [8]. $\frac{1}{S}\frac{\mathrm{d}N}{\mathrm{d}y}$ values are calculated using the appropriate $S_\perp^{\text{var}}$ and $\frac{\mathrm{d}N}{\mathrm{d}y}$ columns from Table I of Ref. [41]. Each dataset is fit separately with a linear function.

where most energy loss occurs before the parton traverses the full path length. Thereby, medium density becomes the dominant factor that determines the energy loss during the rapid expansion. Recent theoretical studies also suggest that the formation time of partons could play a strong role in determining the medium-induced energy loss [43]. We argue that in such a rapidly expansive medium, the static path length from the initial geometry of colliding nuclei fails to be the dominating factor for the parton energy loss in the medium.

Due to limited statistics across multiple centralities, it is challenging to perform a similar measurement for the heavy-flavor hadrons studied here. Recent theoretical models incorporating both collisional and radiative energy loss mechanisms predict a constant value of $\Delta p_T/p_T$ beyond $p_T \sim 5$ GeV/c for charmed hadrons in various collision systems at LHC energies [44]. This would disagree with the rising p_T trends observed in the D^0 and J/ψ R_{AA} data in this study, which point to p_T-dependent fractional energy loss in LHC data, unlike RHIC data. Although these trends are less prominent in the two muons from heavy quark R_{AA} fits, we expect this is due to the decay kinematics of those measurements, which may obscure the expected rising trend. Leading hadron measurements provide a much cleaner measurement; thus, we argue that the predicted flat fractional energy loss trends from these models undervalue the weight of radiative energy loss,

which would likely produce the observed rising trends. These discrepancies highlight the importance of future heavy-flavor R_{AA} measurements at sPHENIX and LHC to investigate these effects further.

Our parton energy loss scenario predicts that the elliptic flow (v_2) of jets or high-p_T leading particles in $A+A$ collisions of intermediate centrality, if measured with minimal nonflow effects, will be close to zero and significantly smaller than values calculated assuming a static path-length dependence. Therefore, it is challenging to explain the large v_2 values observed for jets and leading particles at high p_T [45–46]. However, previous calculations of nuclear modification factor and anisotropic flow values for jets at RHIC and LHC do not prevent this possibility. In Ref. [47], a wide variety of energy loss models are shown to be able to describe available RHIC and LHC data within experimental uncertainty for both strong and weak path-length-dependent models. While this study indicates that the absence of path-length dependence is disfavored in the explored models inspired by quantum chromodynamics, it does not constrain the path-length-dependent parameter to be larger than zero [47]. The exact degree of path-length dependence of parton energy loss remains an outstanding physics issue, which should be addressed with more precise data. It is puzzling why the observed v_2 for jets or leading particles shows a weak p_T dependence, while the magnitude of parton energy loss exhibits a strong p_T dependence. There are some experimental details worthy of further investigation, such as the subtraction scheme for the v_2-dependent background. The nonflow correlations in elliptic flow measurements for jets and high-p_T particles present an important factor to be accounted for as well. These experimental concerns should be adequately addressed before the path length dependence of the parton energy loss may be definitively determined.

V. CONCLUSIONS

In summary, we present a parton energy loss study showing a significant distinction between RHIC and LHC data when empirically interpreting $R_{AA}(p_T)$ as a momentum loss in $A+A$ collisions relative to the $p+p$ reference. While the RHIC data favor a direct proportionality between the p_T shift and p_T itself, the LHC data suggest a proportionality with $\sqrt{p_T}$. This difference in the p_T dependence signifies the heightened importance of radiative energy loss compared with collisional energy loss within the same transverse momentum range in colliding systems at higher $\sqrt{s_{NN}}$. Additionally, we find that the magnitude of the parton energy loss at LHC is largely determined by the initial medium entropy density, which is consistent with previous results at RHIC. This indicates that the path-length dependence of parton energy loss is less dominant, placing a greater emphasis on the initial medium density for a rapidly expanding medium. The distinct parton energy loss dynamics at RHIC and LHC can be further investigated with high-statistics heavy-quark-tagged jets from the sPHENIX experiment at RHIC, as well as LHC experiments in future runs. The possible sequential treatment of fragmentation and parton energy loss is of great interest for these future experiments. Equally interesting is the differentiation of energy loss contributions from quarks and gluons for the measurements studied here.

References

[1] H. van Hees and R. Rapp, Phys. Rev. C **71**, 034907 (2005)

[2] G. D. Moore and D. Teaney, Phys. Rev. C **71**, 064904 (2005)

[3] M. G. Mustafa, Phys. Rev. C **72**, 014905 (2005)

[4] A. Adil, M. Gyulassy, W. Horowitz *et al.*, Phys. Rev. C **75**, 044906 (2007)

[5] Y. L. Dokshitzer and D. E. Kharzeev, Phys. Lett. B **519**, 199 (2001)

[6] A. Adil and M. Gyulassy, Phys. Lett. B **602**(1), 52 (2004)

[7] I. Vitev, Phys. Lett. B **639**(1), 38 (2006)

[8] G. Wang and H. Z. Huang, Phys. Lett. B **672**(1), 30 (2009)

[9] K. Adcox, S. Adler, S. Afanasiev *et al.*, Nucl. Phys. A **757**(1), 184 (2005)

[10] A. Adare, S. Afanasiev, C. Aidala *et al.*, Phys. Rev. C **93**, 024901 (2016)

[11] M. Gyulassy, P. Levai, and I. Vitev, Nucl. Phys. B **594**(1), 371 (2001)

[12] A. V. Sadofyev, M. D. Sievert, and I. Vitev, Phys. Rev. D **104**(9), 094044 (2021)

[13] G. Aad, B. Abbott, K. Abeling *et al.*, Phys. Lett. B **846**, 138154 (2023)

[14] W. Chen, S. Cao, T. Luo *et al.*, Phys. Lett. B **777**, 86 (2018)

[15] K. Adcox, S. S. Adler, N. N. Ajitanand *et al.*, Phys. Rev. Lett. **86**, 3500 (2001)

[16] B. B. Back, M. D. Baker, D. S. Barton *et al.*, Phys. Rev. C **65**, 031901 (2002)

[17] I. Bearden *et al.* (BRAHMS Collaboration), Phys. Lett. B **523**, 227 (2001)

[18] B. I. Abelev, M. M. Aggarwal, Z. Ahammed *et al.*, Phys. Rev. C **79**, 034909 (2009)

[19] J. Adams *et al.* (STAR Collaboration), Phys. Rev. Lett. **91**, 172302 (2003)

[20] B. I. Abelev *et al.* (STAR Collaboration), Phys. Rev. Lett. **98**, 192301 (2007)

[21] S. S. Adler *et al.* (PHENIX Collaboration), Phys. Rev. C **76**, 034904 (2007)

[22]   A. Adare, S. Afanasiev, C. Aidala, *et al*., Phys. Rev. Lett. **101**(16), 162301 (2008)

[23]   B. Abelev *et al*. (The ALICE Collaboration), Eur. Phys. J. C **73**, 2456 (2013)

[24]   S. Acharya, D. Adamovxa, M. M. Aggarwal *et al*., Eur. Phys. J. C **77**, 1 (2017)

[25]   S. Acharya, D. Adamovxa, S. P. Adhya *et al*., Phys. Rev. C **101**, 044907 (2020)

[26]   A. M. Sirunyan, *et al*., Eur. Phys. J. C **78**(6), 509 (2018)

[27]   A. Sirunyan, A. Tumasyan, W. Adam *et al*., Phys. Lett. B **782**, 474 (2018)

[28]   G. Aad, B. Abbott, D. Abbott *et al*., Phys. Lett. B **829**, 137077 (2022)

[29]   C.-Y. Wong and G. Wilk, Acta Phys. Polon. B **43**(11), 2047 (2012)

[30]   B. Abelev, J. Adam, D. Adamovxa, *et al*., Phys. Lett. B **720**(1), 52 (2013)

[31]   S. Acharya *et al*.(ALICE Collaboration), Phys. Rev. C **98**, 044901 (2018)

[32]   S. K. Das, J. M. Torres-Rincon and R. Rapp, Phys. Rept. **1129-1131**, 1 (2025)

[33]   M. Spousta and B. Cole, Eur. Phys. J. C **76**(2), 50 (2025)

[34]   R. Baier, Y. L. Dokshitzer, A. H. Mueller *et al*., JHEP **2001**(09), 033 (2001)

[35]   A. Buzzatti and M. Gyulassy, Nuclear Physics A **904-905**, 779c (2013)

[36]   S. Acharya *et al*. (ALICE Collaboration), Nature **605**(7910), 440 (2022)

[37]   A. M. Sirunyan, A. Tumasyan, W. Adam *et al*., Phys. Rev. Lett. **123**, 022001 (2019)

[38]   S. Acharya, D. Adamovxa, A. Adler *et al*., JHEP **2020**, 141 (2020)

[39]   S. Y. Chen, J. Yan, W. Dai *et al*., Chin. Phys. C **46**(10), 104102 (2022)

[40]   L. H. Song, L. W. Yan and C. G. Duan, Chin. Phys. C **41**(2), 023102 (2017)

[41]   M. Petrovici, A. Lindner, A. Pop, *et al*., Phys. Rev. C **98**, 024904 (2018)

[42]   J. W. Harris and B. Müller, Eur. Phys. J. C **84**(3), 247 (2024)

[43]   M. Zhang, Y. He, S. Cao, *et al*., Chin. Phys. C **47**(2), 024106 (2023)

[44]   J. Zhao, J. Aichelin, P. B. Gossiaux, *et al*., Phys. Rev. C **111**, 014907 (2025)

[45]   R. Snellings, J. Phys. G **41**(12), 124007 (2014)

[46]   J. Chen, J. H. Chen, X. Dong *et al*., Nucl. Sci. Tech. **35**(12), 214 (2024)

[47]   M. Gary, D. Grumiller, S. Prohazka *et al*., JHEP **2014**(08), 001 (2014)